TISSUE ENGINEERING
Volume 12, Number 12, 2006

Development of Controlled Matrix Heterogeneity on a Triphasic Scaffold for Orthopedic Interface Tissue Engineering

JEFFREY P. SPALAZZI, M.S.,[1] STEPHEN B. DOTY, Ph.D.,[2] KRISTEN L. MOFFAT, M.S.,[1] WILLIAM N. LEVINE, M.D.,[3] and HELEN H. LU, Ph.D.[1,4]

ABSTRACT

Biological fixation of orthopedic soft tissue grafts to bone poses a significant clinical challenge. The clinical success of soft tissue–based grafts for anterior cruciate ligament (ACL) reconstruction is limited by the lack of functional graft integration with subchondral bone. Soft tissues such as the ACL connect to subchondral bone via a complex interface whereby three distinct tissue regions (ligament, fibrocartilage, and bone) work in concert to facilitate load transfer from soft to hard tissue while minimizing stress concentration at the interface. Although a fibrovascular tissue forms at the graft-to-bone interface following surgery, this tissue is nonphysiologic and represents a weak link between the graft and bone. We propose that the re-establishment of the native multi-tissue interface is essential for biological graft fixation. *In vivo* observations and our *in vitro* monolayer co-culture results suggest that osteoblast-fibroblast interaction is important for interface regeneration. This study focuses on the design of a triphasic scaffold system mimicking the multi-tissue organization of the native ACL-to-bone interface and the evaluation of osteoblast-fibroblast interactions during three-dimensional co-culture on the triphasic scaffold. We found that the triphasic scaffold supported cell proliferation, migration and phenotypic matrix production while maintaining distinct cellular regions and phase-specific extracellular matrix deposition over time. This triphasic scaffold is designed to guide the eventual reestablishment of an anatomically oriented and mechanically functional fibrocartilage interfacial region directly on biological and synthetic soft tissue grafts. The results of this study demonstrate the feasibility of multi-tissue regeneration on a single scaffold, and the potential of interface tissue engineering to enable the biological fixation of soft tissue grafts to bone.

INTRODUCTION

THE ANTERIOR CRUCIATE LIGAMENT (ACL) is the primary knee joint stabilizer and the most frequently injured knee ligament, with approximately 100,000 reconstruction procedures performed each year in the United States.[1–5] Because of the poor healing potential of the ACL,[6] surgical reconstruction is necessary to restore normal knee function. The long-term performance of ACL reconstruction grafts depends on the structural and material properties of the graft, the initial graft tension,[7–12] the intra-articular position of the graft,[13,14] graft fixation,[15,16] and optimized postoperative rehabilitation.

Autologous hamstring tendon-based grafts are increasingly used for ACL reconstruction because of the high incidence of donor site morbidity associated with bone-patellar

[1]Biomaterials and Interface Tissue Engineering Laboratory, Department of Biomedical Engineering, Columbia University, New York, New York.
[2]Analytical Microscopy Core Laboratory, Hospital for Special Surgery, New York, New York.
[3]Department of Orthopaedic Surgery, Columbia University, New York, New York.
[4]College of Dental Medicine, Columbia University, New York, New York.

tendon-bone grafts.[17,18] Clinically, the hamstring tendon graft is mechanically fixed within the femoral bone tunnel with a cross-pin, while a fixation screw is used to secure the graft within the tibial bone tunnel. While these grafts may restore the physiologic range of motion and joint function through mechanical fixation, biological fixation is not achieved because disorganized scar tissue forms within the bone tunnels. The native fibrocartilage insertion site fails to regenerate following surgery with traditional reconstruction techniques and mechanical fixation methods.[19] Without a functional interface, the graft-bone junction exhibits limited mechanical stability,[15,16,20] and the lack of graft integration constitutes the primary cause of graft failure.[15,16,21–23]

Soft tissues such as tendons or ligaments connect to bone through a characteristic fibrocartilage interface, with controlled spatial variation in cell type and matrix composition. Three distinct tissue regions are observed: ligament, fibrocartilage, and bone.[24–32] The fibrocartilage region is further divided into nonmineralized and mineralized fibrocartilage zones. The ligament proper is composed of fibroblasts embedded in a type I and type III collagen matrix. The nonmineralized fibrocartilage matrix is composed of ovoid chondrocytes, and type II collagen is present within the proteoglycan-rich matrix. The mineralized fibrocartilage consists of hypertrophic chondrocytes surrounded by a calcified matrix,[30] and type X collagen is detected only within this region.[28] The last region is the subchondral bone, within which osteoblasts, osteocytes, and osteoclasts are embedded in a mineralized type I collagen matrix. This controlled matrix heterogeneity likely permits a gradual transition of mechanical load between soft tissue and bone, and in turn minimizes the formation of stress concentrations.[25,33]

Increased emphasis has been placed on graft fixation since postoperative rehabilitation protocols require the immediate ability to regain full range of motion, re-establish neuromuscular function, and bear weight.[19,34] However, the mechanisms governing interface regeneration are not well understood. While tendon-to-bone healing following ACL reconstruction with hamstring tendon grafts does not lead to the re-establishment of the native insertion, fibrovascular tissue is consistently formed within the bone tunnels.[19,35–46] Furthermore, Fujioka *et al.*[47] reported that cellular reorganization occurred at the site of surgical reattachment of the Achilles tendon, along with the formation of nonmineralized and mineralized fibrocartilage-like regions. These reports collectively suggest that interactions between cells derived from tendon (i.e., fibroblasts) and bone tissue (i.e., osteoblasts) may play a significant role in interface regeneration.

We propose that functional biological integration of soft tissue–based ACL reconstruction grafts with bone may be achieved through the regeneration of the native fibrocartilage interface. Previous work from our laboratory evaluating the interaction of osteoblasts and fibroblasts in a monolayer co-culture model revealed that co-culture modulated cellular phenotype, resulting in a decrease in osteoblast alkaline phosphatase activity and the expression of type II collagen, as well as an increase in the mineralization potential of fibroblasts.[48] In addition, Nawata *et al.*[49] reported that postnatal reorganization of the ACL-to-bone insertion may involve the transdifferentiation of fibroblasts into fibrochondrocytes.

On the basis of these observations, it is clear that interface regeneration will require controlled cell-to-cell interactions. Therefore, we propose that the ideal scaffold for interface tissue engineering must support multi-tissue regeneration, promote homotypic and heterotypic cell interactions, and facilitate the development of distinct cellular and matrix zones mimicking those of the native insertion.[50] In addition to supporting cell attachment and growth, each phase of the scaffold should be designed to ensure that controlled morphologic and chemical stimuli are present to promote phase- and tissue-specific matrix elaboration. As with other tissue engineering applications, the interface scaffold must be biodegradable and exhibit mechanical properties comparable to those of the native ligament-to-bone insertion site.

This study focuses on the design and *in vitro* evaluation of a multiphasic scaffold with the potential to direct the regeneration of the multi-tissue interface between tendon grafts and bone. Our working hypothesis is that osteoblast and fibroblast interactions on a three-dimensional, biomimetic scaffold will lead to the development of distinct matrix organization on a continuous scaffold. The first objective of this study was to design a multiphasic scaffold mimicking the native ACL-to-bone interface. The second objective was to establish the feasibility of co-culturing osteoblasts and fibroblasts on the scaffold while maintaining distinct cellular regions. The final objective was to determine the effect of osteoblast and fibroblast interaction on the development of controlled matrix heterogeneity on the multiphasic scaffold. It was anticipated that the multiphasic scaffold design and controlled osteoblast-fibroblast interactions would result in distinct cellular zones and interface-relevant matrix organization on a single construct, building the foundation for the development of functional fixation devices with the potential to facilitate biological graft fixation.

MATERIALS AND METHODS

Objective I: scaffold design and characterization

Mimicking the matrix organization and the three distinct tissue types present at the native ACL insertion, the triphasic scaffold designed for this study consists of three phases (Fig. 1): Phase A for soft tissue, Phase B for the development of the fibrocartilage region, and Phase C for bone. A triphasic and continuous scaffold was fabricated in four stages. First, Phase A was formed from polyglactin 10:90 knitted mesh sheets (Vicryl VKML, Ethicon, Somerville, NJ) by sintering segments of the polymer mesh in cylindrical molds at 150°C for 20 h. Phase B consisted of poly(D-L-lactide-co-glycolide) 85:15 copolymer (PLGA, $M_w \approx 123.6$ kDa;

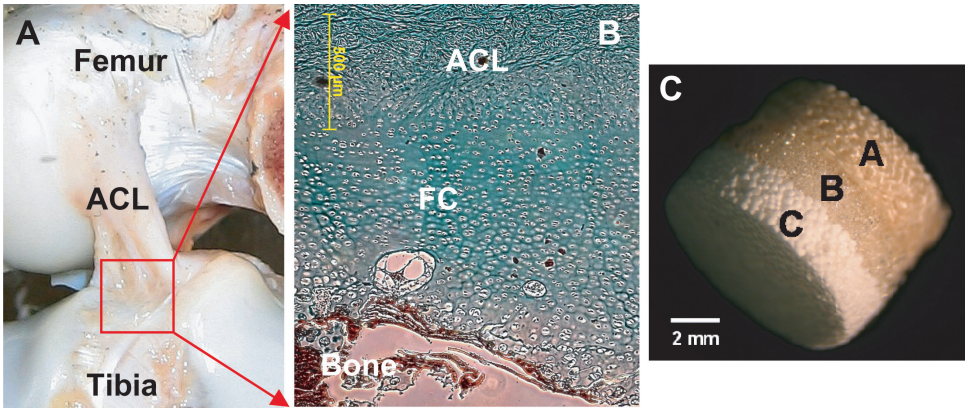

FIG. 1. Design of biomimetic triphasic scaffold. (**A**) Posterior view of bovine anterior cruciate ligament (ACL) with the tibial ACL insertion into bone outlined. (**B**) Histologic image of neonatal bovine tibial ACL insertion showing the three main tissue types found at the ACL-bone interface: ligament, fibrocartilage (FC), and bone (modified Goldner Masson's trichrome stain). (**C**) Triphasic scaffold mimicking the three tissue regions found at the interface.

Alkermes, Cambridge, MA) microspheres formed by a water/oil/water emulsion.[51] Briefly, PLGA was first dissolved in dichloromethane (10% w/v, EM Science, Gibbstown, NJ), then poured into a 1% polyvinyl alcohol solution (Sigma, St. Louis, MO) to form the PLGA microspheres. Phase B was fabricated by sintering the microspheres above the polymer glass transition temperature for 5 h. Phase C was comprised of composite microspheres consisting of a 4:1 ratio of PLGA and 45S5 bioactive glass (BG, 20 μm; Mo-Sci Corp., Rolla, MD), and the PLGA-BG microspheres were sintered for 5 h to form Phase C.[52] Phases A and B were joined together and subsequently sintered onto Phase C by heating all three phases together. The triphasic scaffolds were sterilized with ethylene oxide and vacuum desiccated for 24 h before characterization and *in vitro* evaluation.

Total scaffold diameter and thickness were measured following fabrication. Individual phase thickness ($n = 15$) was determined by image analysis (ImageJ, version 1.34s, National Institutes of Health, Bethesda, MD), while phase diameter ($n = 5$) was measured using a digital caliper. Scaffold porosity and pore diameter were evaluated by mercury porosimetry ($n = 3$; Micromeritics, Norcross, GA).

Objective II: cell localization and maintenance of distinct cellular regions

Cells and cell culture. Primary bovine fibroblasts and osteoblasts were obtained from, respectively, explant cultures of ACL and trabecular bone tissue according to methods described elsewhere.[53,54] For osteoblast outgrowth, trabecular bone chips were isolated from subchondral bone using a bone rongeur. The bone chips were first rinsed thoroughly with phosphate-buffered saline (PBS, Sigma Chemicals, St. Louis, MO) to remove the bone marrow, then cultured in Dulbecco's modified Eagle medium (DMEM) supplemented with 10% fetal bovine serum, 1% nonessential amino acids, and 1% penicillin/streptomycin. For the fibroblast cultures, the ligament tissue was minced and incubated in fully supplemented DMEM. Only cells obtained from second migration were used to ensure a relatively homogenous cell population.[53] All media and supplements were purchased from Mediatech (Herndon, VA).

Localization of osteoblast-fibroblast co-culture on the triphasic scaffolds. To determine cell localization on the triphasic scaffold, primary osteoblasts were seeded on Phase C (2×10^5 cells/phase). The cells were permitted to attach for 30 min before the addition of media. After 24 h, fibroblasts were seeded on Phase A of the triphasic scaffold (2×10^5 cells/phase). Osteoblasts and fibroblasts were co-cultured on the scaffold for 4 weeks, and the media was supplemented with 10 μg/mL ascorbic acid and 3 mM β-glycerophosphate beginning at day 7.

Cell attachment, migration, and growth on the triphasic scaffolds were evaluated by fluorescence microscopy over the 4-week period. To monitor cell distribution and migration, osteoblasts were prelabeled with CM-DiI (2 μM) cell tracking membrane dye (Molecular Probes, Eugene, OR) before seeding, and all cells were subsequently labeled with calcein AM (8 μM) viability dye (Molecular Probes) following the manufacturer's protocols. The samples were imaged at day 0 and 28 using fluorescence microscopy (Carl Zeiss Inc., Thornwood, NY).

Objective III: development of controlled matrix heterogeneity on the triphasic scaffold

Cells and cell culture. Human osteoblast-like cells and fibroblasts were obtained from explant cultures of tissue isolated from humeral trabecular bone and hamstring tendon, respectively. The human tissue samples were obtained as surgical waste following ACL reconstruction surgery and were exempted from institutional review board approval. Briefly, the trabecular bone chips were rinsed thoroughly

with PBS and then cultured in fully supplemented DMEM; cell outgrowth was monitored over time. The tendon tissue was minced and cultured in similarly supplemented DMEM. Only cells obtained from second and third migrations were used in planned experiments to ensure a relatively homogenous cell population.[53]

Osteoblast-fibroblast co-culture on triphasic scaffolds. After establishing the feasibility of osteoblast-fibroblast co-culture on the triphasic scaffold, the effects of cell-cell interactions on the development of controlled matrix heterogeneity was evaluated. Specifically, human hamstring tendon fibroblasts (1.1×10^4 cells/cm^2) were seeded on Phase A. After the cells were allowed to attach for 30 min, primary human osteoblasts (1.1×10^4 cells/cm^2) were seeded on Phase C of the triphasic scaffold. On the basis of porosimetry analysis, total surface area of Phase A was approximately three times greater than that of Phase C. Consequently, three times more cells were seeded on Phase A than Phase C. After the osteoblasts were allowed to attach for 30 min, supplemented DMEM was added and the samples were incubated at 37°C under humidified conditions. Ascorbic acid (20 μg/mL) was added beginning at day 7, and no β-glycerophosphate was added in this experiment to prevent ectopic mineralization of the fibroblasts on Phase A. Each well was precoated with agarose to limit cell migration, and media was exchanged regularly.

Cell proliferation, gene expression, alkaline phosphatase (ALP) activity, and extracellular matrix production were determined as a function of scaffold phase and culturing time. Compressive mechanical properties of the co-cultured triphasic scaffold were measured over time, with acellular scaffolds as controls.

Cell proliferation. Cell proliferation ($n=5$) was determined at days 1, 7, 21, and 35 by measuring total DNA per scaffold phase using the PicoGreen double-stranded DNA assay (Molecular Probes) following the manufacturer's suggested protocol.[55] At designated time points, each triphasic scaffold was rinsed with PBS and the three phases were separated using a scalpel. The cells in each phase were lysed with 0.1% Triton-X solution (Sigma), and each phase was homogenized (Biospec, Bartlesville, OK). Fluorescence of the samples was measured with a microplate reader (Tecan, Research Triangle Park, NC), with excitation and emission wavelengths of 485 and 535 nm, respectively. The total number of cells in the sample was determined by converting the amount of DNA per sample to cell number using the conversion factor of 8 pg DNA/cell.[56]

Gene expression. We measured gene expression by using reverse transcription polymerase chain reaction (RT-PCR) at day 42. The three phases were separated and homogenized, and total RNA was isolated using the Trizol extraction method (Invitrogen, Carlsbad, CA). The isolated RNA was reverse-transcribed into complementary DNA (cDNA) using the SuperScript First-Strand Synthesis System (Invitrogen), and the cDNA product was amplified using recombinant Taq DNA polymerase (Invitrogen). Expression of glyceraldehyde-3-phosphate dehydrogenase (GAPDH) (GAPDH sense, 5′-GGTGATGCTGGTGCTGAGTA-3′; antisense, 5′-ATCCACAGTCTTCTGGGTGG-3′, 305 base pairs) and type I collagen (type I collagen sense, 5′-TGC TGGCCAACCATGCCTCT-3′; antisense, 5′-TTGCACAA TGCTCTGATC-3′, 489 base pairs) were determined. All genes were amplified for 40 cycles in a thermocycler (Eppendorf Mastercycler gradient, Brinkmann, Westbury, NY). Type I collagen band intensities were measured and normalized against GAPDH (ImageJ).

Alkaline phosphatase activity. Sample ALP ($n=5$) activity was determined using an enzymatic assay based on the hydrolysis of p-nitrophenyl phosphate (pNP-PO_4) to pNP.[55,57] Aliquots of the sample homogenate (25 μL) were added to 75 μL of 10 mM pNP-PO_4 and were incubated at 37°C for 30 min. The reaction was terminated by addition of 100 μL of 0.1 N sodium hydroxide, and sample absorbance was measured at 415 nm using a microplate reader (Tecan).

Cell attachment and phase-dependent extracellular matrix deposition in co-culture. Cell attachment morphology and growth on each phase of the triphasic scaffold ($n=2$) were examined immediately following seeding and at days 7, 21, and 35 using scanning electron microscopy (SEM, 3 kV; JEOL 5600LV, Tokyo, Japan, and FEI Quanta 600, FEI Co., Hillsboro, OR). The triphasic scaffold was rinsed in buffer and fixed with Karnovsky's fixative[58,59] for 24 h at 4°C and was dehydrated with an ethanol series. The scaffolds were mounted on an aluminum post and were gold-coated before analysis to reduce charging effects. Matrix distribution on each phase of the scaffold was monitored using SEM after 7, 21, and 35 days of culture. Elemental composition of the elaborated matrix on each phase was determined for non-gold coated samples using energy dispersive x-ray analysis (EDAX, 15 kV; FEI Quanta 600).

Scaffold mechanical properties. Compressive mechanical properties of the samples ($n=4$) were determined at days 0, 7, 21, and 35. The samples were tested under uniaxial compression (MTS 810, Eden Prairie, MN) following the methods of Lu *et al.*[52] Phase A was removed before testing since this phase is intended for soft tissue formation, and therefore the compressive properties of this phase are less relevant than those of Phase B and Phase C. Moreover, Phase A degraded rapidly over the 5-week period, and removal of this phase standardized the testing method. The samples were tested at a displacement rate of 1.3 mm/min following a 10-N preload.[60] A stress-strain curve was generated and compressive modulus was determined by calculating the slope of the elastic region of the stress-strain curve.

Table 1. Summary of Postfabrication Characterization of Each Phase of the Triphasic Scaffold*

Phase	*Composition*	*Height (mm)*	*Diameter (mm)*	*Intrusion Volume (μL)*	*Porosity (%)*	*Mode Pore Diameter (μm)*
A	10:90 PLGA	2.44 ± 0.14	6.75 ± 0.12	41 ± 8	58 ± 5	73 ± 11
B	85:15 PLGA	2.2 ± 0.2	7.32 ± 0.08	28 ± 7	34 ± 4	75 ± 7
C	80% 85:15 PLGA, 20% BG	1.5 ± 0.2	6.5 ± 0.4	14.5 ± 0.1	26.7 ± 0.4	62 ± 3

Abbreviations: BG, bioactive glass; PLGA, poly(D-L-lactide-co-glycolide).
*Values are expressed as the mean ± standard deviation.

Statistical analysis

Results are presented in the form of mean ± standard deviation, with *n* equal to the number of samples analyzed. A two-way analysis of variance (ANOVA) was performed to determine scaffold phase and temporal effects on total cell number and ALP activity. Similarly, two-way ANOVA was performed to determine effects of co-culture and time on scaffold compressive modulus. The Tukey-Kramer *post hoc* test was performed for all pairwise comparisons and statistical significance was attained at a *p* value less than .05. All statistical analyses were performed using JMP statistical software (SAS Institute, Cary, NC).

RESULTS

Objective I: biomimetic scaffold design and characterization

Because the native ligament-to-bone interface (Fig. 1-B) consists of three distinct yet continuous tissue regions—ligament, fibrocartilage, and bone—we designed a triphasic scaffold (Fig. 1-C) with the potential to support the simultaneous formation of these three types of tissue. Phase A of the triphasic scaffold is intended for fibroblast culture and soft tissue formation, while Phase C is intended for osteoblasts and bone formation. The intermediate region, Phase B, will support the co-culture of osteoblasts and fibroblasts and will promote the development of a fibrocartilage-like interface.

Specifically, Phase A consists of a polymer fiber mesh intended for fibroblast attachment and matrix production, Phase C consists of a polymer-bioactive glass composite previously shown to be osteoconductive,[52,61] and Phase B consists of a porous polymer intermediate region where the two cell types can interact and potentially form a fibrocartilaginous zone. Properties of the as-fabricated scaffold are summarized in Table 1. The average thickness of Phases A, B, and C were 2.44 ± 0.14 mm, 2.2 ± 0.2 mm, and 1.5 ± 0.2 mm, and the mean phase diameters were 6.75 ± 0.12 mm, 7.32 ± 0.08 mm, and 6.5 ± 0.4 mm, respectively. Scaffold porosity varied between 25% and 60% depending on the phase, and mode pore diameter remained relatively constant throughout the scaffold at approximately 70 μm. The compressive modulus of the as-fabricated scaffold was 110 ± 20 MPa.

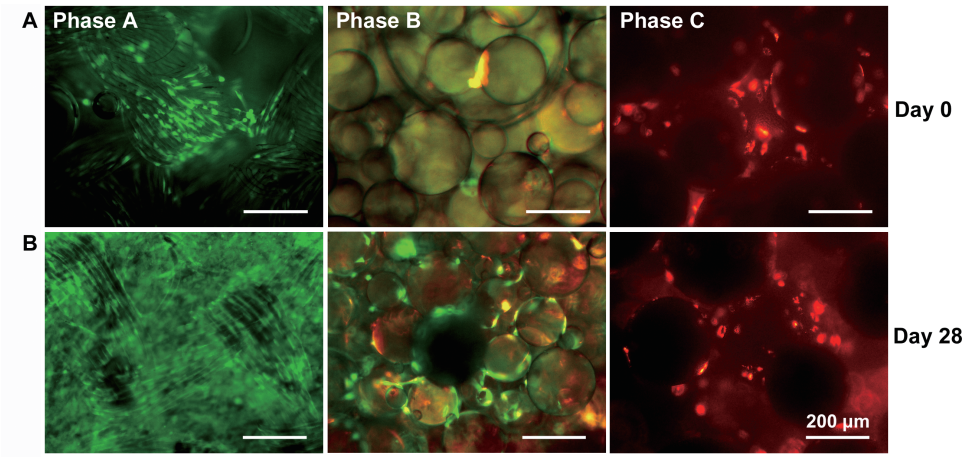

FIG. 2. Phase-specific cell distribution on the triphasic scaffold. (**A**) Fluorescence microscopy revealed that at day 0, fibroblasts (labeled with calcein AM, *green*) attached primarily to Phase A and osteoblasts (labeled with CM-DiI, *red*) to Phase C, with very few cells found in Phase B. (**B**) After 28 days of co-culture, fibroblasts remained localized on Phase A and osteoblasts on Phase C, while both cell types migrated into Phase B. Cell growth and matrix elaboration were observed on all three phases. (Bar = 200 μm.)

Objective II: cell localization and migration

To validate the co-culture of osteoblasts and fibroblasts on the three-dimensional scaffold, the second objective of this study was to monitor the migration of both cell types into Phase B over time. As shown in Fig. 2, fluorescence microscopy revealed that fibroblasts (labeled with calcein AM, *green*) and osteoblasts (labeled with CM-DiI, *red*) were indeed localized primarily on their respective phases, with very few cells found in Phase B after initial seeding (Fig. 2A). After 28 days of culture, fibroblasts and osteoblasts proliferated within their respective phases, and both fibroblasts and osteoblasts migrated into Phase B (Fig. 2B). With this scaffold design, osteoblasts and fibroblasts were largely localized in their respective regions, while their interaction was restricted to Phase B at day 28.

Objective III: phase-specific cell proliferation during co-culture

Cell number increased in all scaffold phases over 35 days of co-culture (Fig. 3). The number of fibroblasts on Phase A increased significantly over time. The number of osteoblasts increased on Phase C from day 7 to day 35, but the difference was not statistically significant. The number of cells in Phase B also increased significantly over time, likely resulting from both cell migration and proliferation in Phase B. The highest number of cells was found in Phase A. Because of the greater surface area for cellular attachment in Phase A compared with Phase C, approximately three times more cells were seeded on Phase A to maintain cell seeding density; thus, consistently higher numbers of cells were found in Phase A throughout the 5-week period.

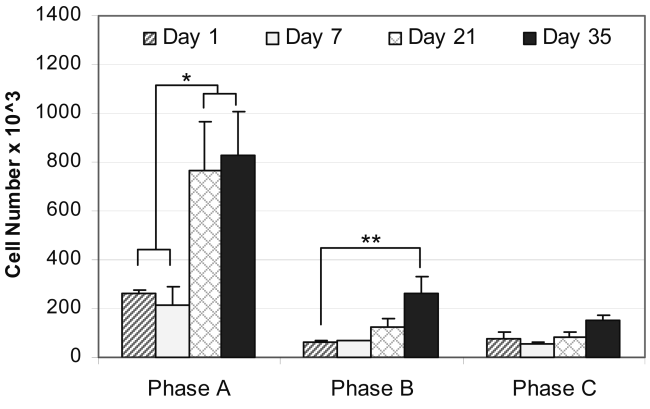

FIG. 3. Cellular proliferation on each phase of the triphasic scaffold. Cell number increased significantly over time on Phase A and Phase B, and there was an increase on Phase C from day 7 to day 35, although this difference was not statistically significant. The increase in cell number on Phase B is attributed to fibroblasts and osteoblasts migrating into this phase and proliferating over time ($n = 5$; $*p < .01$, $**p < .05$).

Objective III: matrix distribution and development of controlled matrix heterogeneity

The third objective of the study was to determine whether localized cell distribution and osteoblast-fibroblast co-culture on the triphasic scaffold would lead to the formation of three distinct matrix regions: Phase A cultured with fibroblasts and with a type I collagen matrix for soft tissue; Phase C cultured with osteoblasts and dominated by a mineralized matrix; and both osteoblasts and fibroblasts restricted to Phase B, where their interaction may result in the production of a fibrocartilage-like matrix. In this study, cell-specific and phase-dependent matrix elaboration was observed throughout the triphasic scaffolds over the culture period. Type I collagen gene expression was detected on Phase A and Phase C at day 42 as expected, whereas type I collagen expression was also detected in cells found on Phase B. This finding indicates the potential for the production of a type I collagen matrix by osteoblasts and fibroblasts in Phase B (Fig. 4). Gene expression for type I collagen was 34% higher in Phase A than in Phase B, and 76% higher in Phase A than in Phase C when normalized to GAPDH expression.

In addition, the highest ALP activity was detected on Phase C, which was seeded with osteoblasts, with a significantly higher level of ALP activity measured at day 7 on this phase ($p < .01$, Fig. 5) compared with the two remaining phases. Only a baseline level of ALP activity was found on Phase A and Phase B over 35 days of culture. The SEM analysis revealed that both fibroblasts and osteoblasts elaborated extracellular matrix on Phases A and C, with cellular migration and matrix formation observed in Phase B (Fig. 6A). At day 28, EDAX analysis revealed that the fibroblasts elaborated a sulfated, protein-rich matrix in Phase A, and a mineralized matrix was only found in Phase C (Fig. 6B).

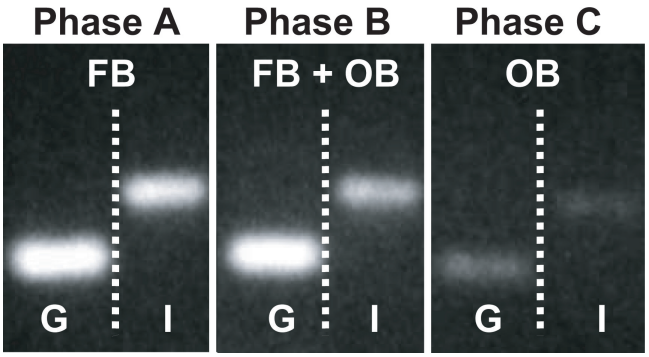

FIG. 4. Phase-specific gene expression of human type I collagen (I) and glyceraldehyde-3-phosphate dehydrogenase (G). Bands indicate expression of type I collagen by fibroblasts (FB) on Phase A, osteoblasts (OB) on Phase C, and FB+OB on Phase B of the triphasic scaffold at day 42.

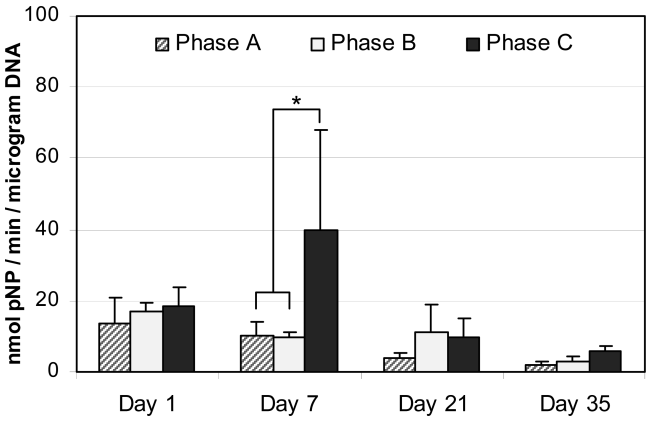

FIG. 5. Phase-specific alkaline phosphatase (ALP) activity on the triphasic scaffold. The ALP activity on Phase C peaked at day 7 and was significantly higher than that on Phase A and Phase B ($n = 5$; $^*p < .01$), indicating that Phase C supports osteoblast differentiation.

Objective III: effects of co-culture on scaffold mechanical properties

The co-cultured scaffolds maintained a higher degree of structural integrity than did the acellular scaffolds. This was evident on Phase A, where the mesh maintained its integrity over time with matrix elaboration by fibroblasts, while this phase was completely degraded in the acellular group by day 35 (Fig. 7A). As the scaffolds degraded over time, compressive modulus significantly decreased *in vitro* ($p < .05$), with a 50% decline in modulus for the seeded scaffold and a 57% decrease for the acellular scaffold after 35 days of culture. While the mean compressive modulus was higher for the co-cultured group, no significant difference was observed between the co-culture and acellular scaffolds.

DISCUSSION

Our long-term research goal is to engineer a functional interface between soft tissue grafts and subchondral bone. The objective of the current study was to test our working hypothesis that controlled matrix heterogeneity can be formed on a triphasic scaffold through biomimetic design and relevant cell-to-cell interactions. Specifically, this study focused on 1) the design and analysis of a triphasic scaffold for interface regeneration, 2) the co-culture of osteoblasts and fibroblasts on the scaffold with the maintenance of distinct cellular zones, and 3) the development of phase- and cell-specific extracellular matrix on the triphasic scaffold.

A biomimetic approach was adopted for scaffold design in this study. The rationale for triphasic scaffold design was to mimic the multi-tissue organization inherent at the native ligament-to-bone insertion site, with each phase corresponding to the tissue type to be regenerated at the insertion. Our goal was to develop distinct yet continuous tissue regions on a single scaffold. To this end, each phase of the scaffold differs in morphology, composition, and cell type. Phase A is designed for soft tissue, while Phase C is designed for bone formation. Phase B is the interfacial region for

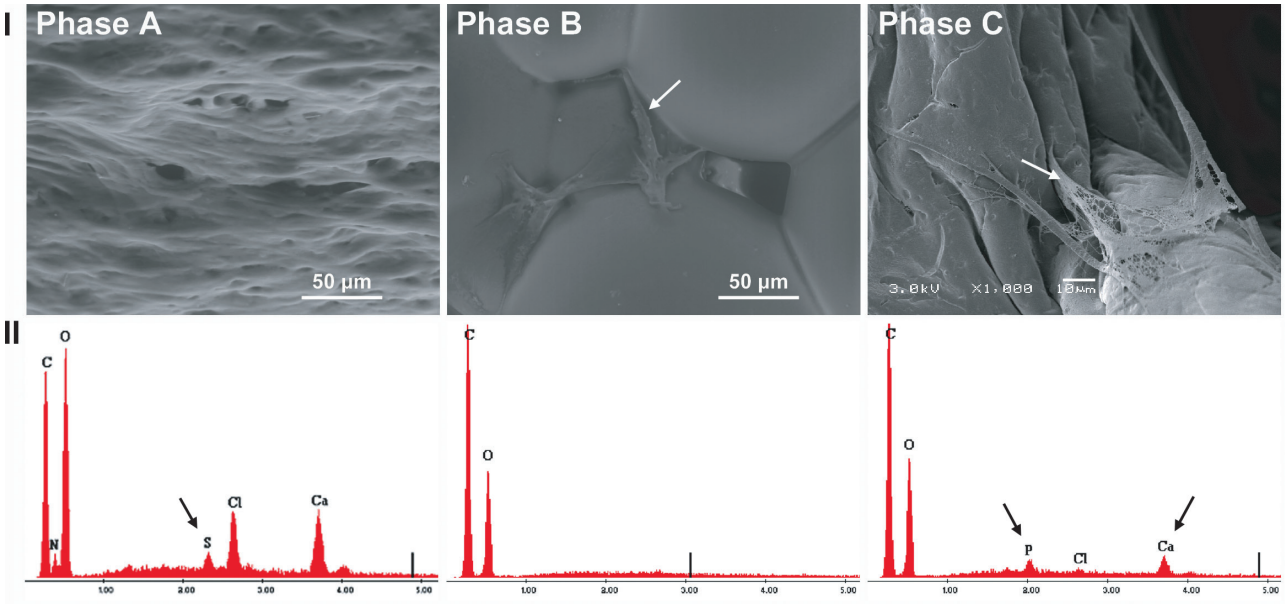

FIG. 6. Development of controlled matrix heterogeneity on the triphasic scaffold. (**A**) Scanning electron microscopy (original magnification, ×1000) revealed extensive matrix formation on Phase A and Phase C (day 35), and cell migration into Phase B (arrow). (**B**) Energy dispersive X-ray analysis revealed that fibroblasts elaborated a sulfated matrix on Phase A, and a mineralized matrix was formed by osteoblasts only on Phase C. Color images available online at www.liebertpub.com/ten.

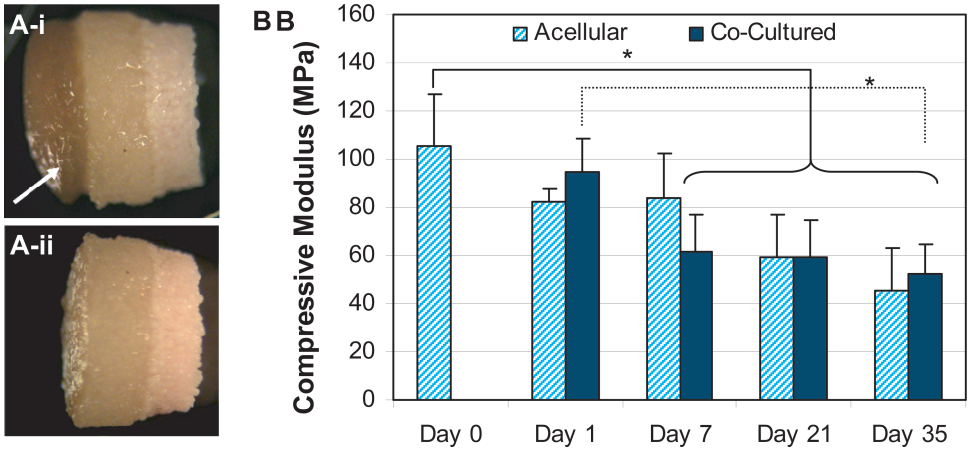

FIG. 7. Mechanical properties and structural integrity of triphasic scaffolds. (**A**) Co-cultured (A-i) and acellular (A-ii) triphasic scaffolds (day 35). Extracellular matrix production compensated for scaffold degradation in the seeded group, whereas Phase A degraded completely in the acellular group. (**B**) Compressive modulus of seeded and acellular triphasic scaffolds over time. Compressive modulus decreased significantly for both groups over time because of scaffold degradation. ($n = 4$; $^*p < .05$). Color images available online at www.liebertpub.com/ten.

heterotypic cell-to-cell interactions and is intended for the eventual regeneration of the fibrocartilage interface. The cell types found on each phase correspond to the insertion region to be regenerated.

It is well established that scaffold chemistry and morphology modulate cell differentiation and matrix elaboration.[53,62–70] Therefore, the triphasic nature of the scaffold is essential for the development of multiple tissue types on a single construct. The scaffold designed for this study include regions with varying morphology as well as chemistry with the specific intention of supporting multiple cell types. The current scaffold system is based on biodegradable polymers and polymer-ceramic composites, including PLGA mesh for Phase A, PLGA polymer microspheres for Phase B, and PLGA-BG composite microspheres for Phase C. A rapidly degrading polymer (PLGA 10:90) was chosen for Phase A to support fibroblast culture on the soft tissue phase, whereas the matrix development necessary on Phase B (PLGA 85:15) and Phase C (PLGA 85:15 and BG) requires long-term scaffold integrity. Polymeric fiber-based scaffolds have been researched extensively for ligament tissue engineering,[53,68,71] and polymer-ceramic composites have been used successfully for bone tissue engineering.[52,72–76] The PLGA-BG composite was selected for the bone phase of the scaffold because of its reported osteointegrative and osteoinductive potential.[61,77–80] While the native fibrocartilage region is divided into nonmineralized and mineralized regions, Phase B in the current scaffold design is composed of PLGA without a mineral component. In adult tissue, the mineralized fibrocartilage zone is narrower than 100 μm, and mineral distribution in this zone is indistinguishable from the bone region.[32] Thus, we elected to focus for now on the formation of a nonmineralized fibrocartilage region in Phase B.

Cell tracking results revealed that following seeding, fibroblasts attached to Phase A and osteoblasts attached to Phase C. After 4 weeks, fibroblasts and osteoblasts continued to proliferate on their respective phases, whereas osteoblast-fibroblast interactions were restricted to Phase B. These observations confirm that the triphasic scaffold design supported the establishment and maintenance of phase-specific cell distribution throughout the scaffold. Cellular proliferation was higher in Phase A and Phase B than in Phase C, most likely because of the difference in proliferation rates between fibroblasts and osteoblasts and the lower porosity of Phase C. Related to the controlled localization of cells, a phase-specific distribution of extracellular matrix was observed in the three phases of the scaffold over time. ALP activity and the elaboration of a mineralized matrix were significantly higher in Phase C, confirming that this phase is osteoconductive *in vitro*. A type I collagen matrix was found in all three phases, including Phase B, and EDAX analysis confirmed abundant extracellular matrix production on Phase A. Phase B is of particular interest because scaffold design enabled localized osteoblast and fibroblast interaction within this interfacial phase. It is anticipated that this direct co-culture of ligament or tendon fibroblasts and osteoblasts may assist in the development of fibrocartilage-specific markers within Phase B, and will be investigated in future studies.

Fibrocartilage is usually localized in regions subjected to compressive loading,[81,82] suggesting that tensile forces in the ACL are distributed to bone through compression and shear in the insertion site.[33] In addition, we previously determined the strain distribution at the ACL-bone insertion using ultrasound elastography and found that when the tibiofemoral joint is loaded in tension, compressive strain exists at the insertion.[83] Consequently, only compressive mechanical properties of Phase B and Phase C were measured in this

study since these phases of the scaffold would be the sites of fibrocartilage and bone formation, respectively, and therefore would be subjected to compressive loading in future clinical application.

Stratified scaffold systems have been researched for orthopedic tissue engineering, and in particular for osteochondral applications.[74,84–88] Schaefer *et al.*[86] seeded bovine articular chondrocytes on polyglycolic acid meshes and periosteal cells on PLGA/polyethylene glycol foams, and subsequently sutured these separate constructs together at 1 or 4 weeks after seeding. Integration between the two scaffolds was observed to be superior when sutured at 1 week, suggesting the importance of cellular interactions immediately after seeding. Similarly, Gao *et al.*[87] seeded mesenchymal stem cell–differentiated chondrogenic cells in a hyaluronan sponge and mesenchymal stem cell–differentiated osteogenic cells in a porous calcium phosphate scaffold. These scaffolds were then joined by fibrin sealant and implanted subcutaneously in syngeneic rats, with continuous collagen fibers observed between the two scaffolds 6 weeks following implantation. In addition, distinct cartilaginous and osseous zones were also formed.

In these pioneering studies on multi-tissue integration, scaffolds with a single cell type were joined after seeding. This process minimized any immediate cellular interactions necessary for eventual construct integration. In addition, scaffold integrity is not optimal in these reported scaffolds because the integration between the two phases is not continuous. In contrast, the triphasic scaffold design used in this study consists of a single continuous construct with integrated phases, upon which cells can interact immediately after seeding. Moreover, osteoblast-fibroblast interaction is localized and promoted within the interface region (Phase B).

To our knowledge, this is the first reported study to focus on developing functional scaffolds and promoting cell-to-cell interactions for regenerating the interface between ligament and bone. The novel triphasic scaffold reported in this study promoted the formation of distinct cellular and matrix regions, and will serve as a model system for developing tissue engineering strategies aimed at regenerating the graft-to-bone interface on soft tissue–based ACL reconstruction grafts. The results of this study demonstrate the feasibility of multi-tissue regeneration on a single graft, with the potential to promote biological fixation of soft tissue grafts to bone.

This triphasic scaffold is designed to guide the eventual reestablishment of an anatomically oriented and mechanically functional fibrocartilage interfacial region directly on both synthetic and biological soft tissue grafts. It is intended to be used clinically as a graft collar for soft tissue graft fixation. In this scenario, Phase C would be inserted into the bone tunnel, while Phases A and B would reside outside the bone tunnel in the joint capsule; cellular interactions will promote the formation of an anatomically oriented and functional fibrocartilage interface. Tensile and torsional forces would be sustained by the soft tissue graft and Phase A. The presence of a physiologic fibrocartilage region will enable the gradual transition of load from the graft to bone,[89] and osteointegration in the bone tunnel will be facilitated by Phase C and the addition of osteogenic factors.

Interface tissue engineering is an emerging field, and biological fixation of soft tissue grafts is a multifaceted problem with many inherent challenges. Through controlled coculture and multiphasic scaffold design, distinct cellular and matrix zones were developed on the triphasic scaffold. The phase-specific cell distribution and matrix heterogeneity were maintained for the duration of the culturing period in this study; however, whether this zonal distribution can be sustained during long-term culture and *in vivo* remains to be seen. Moreover, the mechanisms governing fibrocartilage development or regeneration are not well understood, representing one of the most significant challenges in orthopedic interface tissue engineering. In addition, a prerequisite for biomimetic scaffold design is a clear understanding of the structure-function relationship at the soft tissue-to-bone interface. Results from our ongoing studies in elucidating the mechanisms of interface regeneration and characterization of the chemical and mechanical properties of the ACL-to-bone interface will aid in the optimization of cellular interactions on this multiphasic scaffold. Future studies will focus on strategies for *in vitro* and *in vivo* development of fibrocartilage-specific markers and biomimetic tissue organization on the triphasic scaffold.

In conclusion, we have reported here the design and *in vitro* testing of a triphasic scaffold for soft tissue graft-to-bone integration. The triphasic scaffold supported the growth, migration, and phenotypic matrix production of osteoblasts and fibroblasts. More importantly, this novel biomimetic scaffold supported distinct zonal distributions of cells and phase-specific extracellular matrix deposition over time. This is the first reported study examining the interaction of osteoblasts and fibroblasts on a multiphasic scaffold, and our results demonstrate the feasibility of multi-tissue regeneration on a single construct. The cocultured triphasic scaffold will serve as a model system for formulating tissue engineering strategies for the regeneration of a functional interface on soft tissue reconstruction grafts.

ACKNOWLEDGMENTS

The authors would like to gratefully acknowledge Dr. X. Edward Guo of the Bone Biomechanics Laboratory at Columbia University for his advice on mechanical testing and use of the MTS system, and Dr. Yusuf M. Khan of the University of Virginia and Micromeritics for assistance with porosimetry analysis. This study was funded by National Institutes of Health/National Institute of Arthritis and Musculoskeletal and Skin Diseases (R21 AR052402-01A1) (H.H.L.) an Early Faculty Career Award from the Wallace

H. Coulter Foundation (H.H.L.), and a National Science Foundation Graduate Fellowship (GK-12 0338329) (J.P.S.).

REFERENCES

1. Johnson, R.J. The anterior cruciate: a dilemma in sports medicine. Int. J. Sports Med. **3,** 71, 1982.
2. American Academy of Orthopaedic Surgeons. Arthroplasty and Total Joint Replacement Procedures: United States 1990 to 1997. Rosemont, IL: American Academy of Orthopaedic Surgeons, 1997.
3. Brown, C.H., Jr., and Carson, E.W. Revision anterior cruciate ligament surgery. Clin. Sports Med. **18,** 109, 1999.
4. United States Department of Health and Human Services, Centers for Disease Control and Prevention, National Center for Health Statistics. National Survey of Ambulatory Surgery. Atlanta, GA: Centers for Disease Control and Prevention; 1996.
5. United States Department of Health and Human Services, Centers for Disease Control and Prevention, National Center for Health Statistics. National Hospital Discharge Survey. Atlanta, GA: Centers for Disease Control and Prevention; 1996.
6. Bray, R.C., Leonard, C.A., and Salo, P.T. Vascular physiology and long-term healing of partial ligament tears. J. Orthop. Res. **20,** 984, 2002.
7. Fleming, B., Beynnon, B., Howe, J., McLeod, W., and Pope, M. Effect of tension and placement of a prosthetic anterior cruciate ligament on the anteroposterior laxity of the knee. J. Orthop. Res. **10,** 177, 1992.
8. Gregor, R.J., and Abelew, T.A. Tendon force measurements and movement control: a review. Med. Sci. Sports Exerc. **26,** 1359, 1994.
9. Beynnon, B.D., Yu, J., Huston, D., Fleming, B., Johnson, R., Haugh, L., and Pope, M.H. A sagittal plane model of the knee and cruciate ligaments with application of a sensitivity analysis. J. Biomech. Eng. **118,** 227, 1996.
10. Beynnon, B.D., Johnson, R.J., Fleming, B.C., Peura, G.D., Renstrom, P.A., Nichols, C.E., and Pope, M.H. The effect of functional knee bracing on the anterior cruciate ligament in the weightbearing and nonweightbearing knee. Am. J. Sports Med. **25,** 353, 1997.
11. Fleming, B.C., Abate, J.A., Peura, G.D., and Beynnon, B.D. The relationship between graft tensioning and the anterior-posterior laxity in the anterior cruciate ligament reconstructed goat knee. J. Orthop. Res. **19,** 841, 2001.
12. Fleming, B.C., and Beynnon, B.D. *In vivo* measurement of ligament/tendon strains and forces: a review. Ann. Biomed. Eng. **32,** 318, 2004.
13. Markolf, K.L., Hame, S., Hunter, D.M., Oakes, D.A., Zoric, B., Gause, P., and Finerman, G.A. Effects of femoral tunnel placement on knee laxity and forces in an anterior cruciate ligament graft. J. Orthop. Res. **20,** 1016, 2002.
14. Loh, J.C., Fukuda, Y., Tsuda, E., Steadman, R.J., Fu, F.H., and Woo, S.L. Knee stability and graft function following anterior cruciate ligament reconstruction: comparison between 11 o'clock and 10 o'clock femoral tunnel placement. Arthroscopy **19,** 297, 2003.
15. Robertson, D.B., Daniel, D.M., and Biden, E. Soft tissue fixation to bone. Am. J. Sports Med. **14,** 398, 1986.
16. Kurosaka, M., Yoshiya, S., and Andrish, J.T. A biomechanical comparison of different surgical techniques of graft fixation in anterior cruciate ligament reconstruction. Am. J. Sports Med. **15,** 225, 1987.
17. Beynnon, B.D., Johnson, R.J., Fleming, B.C., Kannus, P., Kaplan, M., Samani, J., and Renstrom, P. Anterior cruciate ligament replacement: comparison of bone-patellar tendon-bone grafts with two-strand hamstring grafts. A prospective, randomized study. J. Bone Joint Surg. Am. **84-A,** 1503, 2002.
18. Barrett, G.R., Noojin, F.K., Hartzog, C.W., and Nash, C.R. Reconstruction of the anterior cruciate ligament in females: a comparison of hamstring versus patellar tendon autograft. Arthroscopy **18,** 46, 2002.
19. Rodeo, S.A., Arnoczky, S.P., Torzilli, P.A., Hidaka, C., and Warren, R.F. Tendon-healing in a bone tunnel. A biomechanical and histological study in the dog. J. Bone Joint Surg. Am. **75,** 1795, 1993.
20. Rodeo, S.A., Suzuki, K., Deng, X.H., Wozney, J., and Warren, R.F. Use of recombinant human bone morphogenetic protein-2 to enhance tendon healing in a bone tunnel. Am. J. Sports Med. **27,** 476, 1999.
21. Friedman, M.J., Sherman, O.H., Fox, J.M., Del Pizzo, W., Snyder, S.J., and Ferkel, R.J. Autogeneic anterior cruciate ligament (ACL) anterior reconstruction of the knee. A review. Clin. Orthop. Relat. Res. **196,** 9, 1985.
22. Jackson, D.W., Grood, E.S., Arnoczky, S.P., Butler, D.L., and Simon, T.M. Cruciate reconstruction using freeze dried anterior cruciate ligament allograft and a ligament augmentation device (LAD). An experimental study in a goat model. Am. J. Sports Med. **15,** 528, 1987.
23. Yahia L. Ligaments and Ligamentoplasties. Berlin Heidelberg: Springer Verlag, 1997.
24. Cooper, R.R., and Misol, S. Tendon and ligament insertion. A light and electron microscopic study. J. Bone Joint Surg. Am. **52,** 1, 1970.
25. Benjamin, M., Evans, E.J., and Copp, L. The histology of tendon attachments to bone in man. J. Anat. **149,** 89, 1986.
26. Wei, X., and Messner, K. The postnatal development of the insertions of the medial collateral ligament in the rat knee. Anat. Embryol. (Berl). **193,** 53, 1996.
27. Sagarriga, V.C., Kavalkovich, K., Wu, J., and Niyibizi, C. Biochemical analysis of collagens at the ligament-bone interface reveals presence of cartilage-specific collagens. Arch. Biochem. Biophys. **328,** 135, 1996.
28. Niyibizi, C., Sagarrigo, V.C., Gibson, G., and Kavalkovich, K. Identification and immunolocalization of type X collagen at the ligament-bone interface. Biochem. Biophys. Res. Commun. **222,** 584, 1996.
29. Messner, K. Postnatal development of the cruciate ligament insertions in the rat knee. morphological evaluation and immunohistochemical study of collagens types I and II. Acta Anatomica. **160,** 261, 1997.
30. Petersen, W., and Tillmann, B. Structure and vascularization of the cruciate ligaments of the human knee joint. Anat. Embryol. (Berl). **200,** 325, 1999.
31. Thomopoulos, S., Williams, G.R., Gimbel, J.A., Favata, M., and Soslowsky, L.J. Variations of biomechanical, structural,

and compositional properties along the tendon to bone insertion site. J. Orthop. Res. **21,** 413, 2003.
32. Wang, I.E., Mitroo, S., Chen, F.H., Lu, H.H., and Doty, S.B. Age-dependent changes in matrix composition and organization at the ligament-to-bone insertion. J. Orthop. Res. **25,** 1745, 2006.
33. Woo, S.L., and Buckwalter, J.A. AAOS/NIH/ORS workshop. Injury and repair of the musculoskeletal soft tissues. Savannah, Georgia, June 18-20, 1987. J. Orthop. Res. **6,** 907, 1988.
34. Brand, J. Jr., Weiler, A., Caborn, D.N., Brown, C.H. Jr., and Johnson, D.L. Graft fixation in cruciate ligament reconstruction. Am. J. Sports Med. **28,** 761, 2000.
35. Grana, W.A., Egle, D.M., Mahnken, R., and Goodhart, C.W. An analysis of autograft fixation after anterior cruciate ligament reconstruction in a rabbit model. Am. J. Sports Med. **22,** 344, 1994.
36. Liu, S.H., Panossian, V., al Shaikh, R., Tomin, E., Shepherd, E., Finerman, G.A., and Lane, J.M. Morphology and matrix composition during early tendon to bone healing. Clin. Orthop. Relat. Res. **339,** 253, 1997.
37. Blickenstaff, K. R., Grana, W.A., and Egle, D. Analysis of a semitendinosus autograft in a rabbit model. Am. J. Sports Med. **25,** 554, 1997.
38. Panni, A.S., Milano, G., Lucania, L., and Fabbriciani, C. Graft healing after anterior cruciate ligament reconstruction in rabbits. Clin. Orthop. **343,** 203, 1997.
39. Eriksson, K., Kindblom, L.G., and Wredmark, T. Semitendinosus tendon graft ingrowth in tibial tunnel following ACL reconstruction: a histological study of 2 patients with different types of early graft failure. Acta Orthop. Scand. **71,** 275, 2000.
40. Yoshiya, S., Nagano, M., Kurosaka, M., Muratsu, H., and Mizuno, K. Graft healing in the bone tunnel in anterior cruciate ligament reconstruction. Clin. Orthop. **376,** 278, 2000.
41. Anderson, K., Seneviratne, A.M., Izawa, K., Atkinson, B.L., Potter, H.G., and Rodeo, S.A. Augmentation of tendon healing in an intraarticular bone tunnel with use of a bone growth factor. Am. J. Sports Med. **29,** 689, 2001.
42. Weiler, A., Hoffmann, R.F., Bail, H.J., Rehm, O., and Sudkamp, N.P. Tendon healing in a bone tunnel. Part II: Histologic analysis after biodegradable interference fit fixation in a model of anterior cruciate ligament reconstruction in sheep. Arthroscopy. **18,** 124, 2002.
43. Thomopoulos, S., Hattersley, G., Rosen, V., Mertens, M., Galatz, L., Williams, G.R., and Soslowsky, L.J. The localized expression of extracellular matrix components in healing tendon insertion sites: an in situ hybridization study. J. Orthop. Res. **20,** 454, 2002.
44. Batra, G.S., Harrison, J.W., Clough, T.M., and Paul, A.S. Failure of anterior cruciate ligament reconstruction following calcification of the graft. Knee **9,** 245, 2002.
45. Chen, C.H., Chen, W.J., Shih, C.H., Yang, C.Y., Liu, S.J., and Lin, P.Y. Enveloping the tendon graft with periosteum to enhance tendon-bone healing in a bone tunnel: a biomechanical and histologic study in rabbits. Arthroscopy **19,** 290, 2003.
46. Song, E.K., Rowe, S.M., Chung, J.Y., Moon, E.S., and Lee, K.B. Failure of osteointegration of hamstring tendon autograft after anterior cruciate ligament reconstruction. Arthroscopy **20,** 424, 2004.
47. Fujioka, H., Thakur, R., Wang, G.J., Mizuno, K., Balian, G., and Hurwitz, S.R. Comparison of surgically attached and nonattached repair of the rat Achilles tendon-bone interface. Cellular organization and type X collagen expression. Connect. Tissue Res. **37,** 205, 1998.
48. Wang, I.E., Jeffries, D.T., Jiang, J., Chen, F.H., and Lu, H.H. Effects of co-culture on ligament fibroblast and osteoblast growth and differentiation. Trans. Orthop. Res. Soc., Paper no. 138, 2004.
49. Nawata, K., Minamizaki, T., Yamashita, Y., and Teshima, R. Development of the attachment zones in the rat anterior cruciate ligament: changes in the distributions of proliferating cells and fibrillar collagens during postnatal growth. J. Orthop. Res. **20,** 1339, 2002.
50. Mikos, A.G., Herring, S.W., Elisseef, J., Lu, H.H., Kandel, R., Schoen, F.J., Toner, M., Mooney, D., Atala, A., Kaplan, D., and Vunjak-Novakovic, G. Engineering complex tissues. Tissue Eng. **12,** 3307, 2006.
51. Borden, M., Attawia, M., Khan, Y., and Laurencin, C.T. Tissue engineered microsphere-based matrices for bone repair: design and evaluation. Biomaterials **23,** 551, 2002.
52. Lu, H.H., El Amin, S.F., Scott, K.D., and Laurencin, C.T. Three-dimensional, bioactive, biodegradable, polymer-bioactive glass composite scaffolds with improved mechanical properties support collagen synthesis and mineralization of human osteoblast-like cells *in vitro*. J. Biomed. Mater. Res. **64A,** 465, 2003.
53. Lu, H.H., Cooper, J.A. Jr., Manuel, S., Freeman, J.W., Attawia, M.A., Ko, F.K., and Laurencin, C.T. Anterior cruciate ligament regeneration using braided biodegradable scaffolds: *in vitro* optimization studies. Biomaterials **26,** 4805, 2005.
54. Spalazzi, J.P., Dionisio, K.L., Jiang, J., and Lu, H.H. Osteoblast and chondrocyte interactions during coculture on scaffolds. IEEE Eng. Med. Biol. Mag. **22,** 27, 2003.
55. Jiang, J., Nicoll, S.B., and Lu, H.H. Co-culture of osteoblasts and chondrocytes modulates cellular differentiation *in vitro*. Biochem. Biophys. Res. Commun. **338,** 762, 2005.
56. Lu, H.H. 45S5 bioactive glass surface zeta potential variations in electrolyte solutions with and without fibronectin [Ph.D. thesis]. Department of Bioengineering, University of Pennsylvania, Philadelphia, Pa, 1998.
57. Teixeira, C.C., Hatori, M., Leboy, P.S., Pacifici, M., and Shapiro, I.M. A rapid and ultrasensitive method for measurement of DNA, calcium and protein content, and alkaline phosphatase activity of chondrocyte cultures. Calcif. Tissue Int. **56,** 252, 1995.
58. Karnovsky, M.J. A formaldehyde-glutaraldehyde fixative of high osmolarity for use in electron microscopy. J. Cell Biol. **27,** 137A, 1965.
59. Langley, S.M., Chai, P.J., Miller, S.E., Mault, J.R., Jaggers, J.J., Tsui, S.S., Lodge, A.J., Lefurgey, A., and Ungerleider, R.M. Intermittent perfusion protects the brain during deep hypothermic circulatory arrest. Ann. Thorac. Surg. **68,** 4, 1999.
60. Standard Test Method for Compressive Properties of Rigid Plastics, Annual Book of ASTM Standards, D 695, 1996, pp. 78–84.
61. Lu, H.H., Tang, A., Oh, S.C., Spalazzi, J.P., and Dionisio, K. Compositional effects on the formation of a calcium phosphate layer and the response of osteoblast-like cells on polymer-bioactive glass composites. Biomaterials **26,** 6323, 2005.

62. Brody, G.A., Eisinger, M., Arnoczky, S.P., and Warren, R.F. *In vitro* fibroblast seeding of prosthetic anterior cruciate ligaments. A preliminary study. Am. J. Sports Med. **16,** 203, 1988.
63. Dunn, M.G., Liesch, J.B., Tiku, M.L., Maxian, S.H., and Zawadsky, J.P. The tissue engineering approach to ligament reconstruction. Proc. Material Res. Soc. **33,** 13, 1994.
64. Bellincampi, L.D., Closkey, R.F., Prasad, R., Zawadsky, J.P., and Dunn, M.G. Viability of fibroblast-seeded ligament analogs after autogenous implantation. J. Orthop. Res. **16,** 414, 1998.
65. Goulet, F., Germain, L., Rancourt, D., Caron, C., Normand, A., and Auger, F.A. Tendons and ligaments. In: Lanza, R.P., Langer, R., and Vacanti, J.P., eds. Principles of Tissue Engineering. San Diego, CA: Academic Press, 2000, pp. 639–645.
66. Altman, G.H., Horan, R.L., Lu, H.H., Moreau, J., Martin, I., Richmond, J.C., and Kaplan, D.L. Silk matrix for tissue engineered anterior cruciate ligaments. Biomaterials **23,** 4131, 2002.
67. Altman, G.H., Lu, H.H., Horan, R.L., Calabro, T., Ryder, D., Kaplan, D.L., Stark, P., Martin, I., Richmond, J.C., and Vunjak-Novakovic, G. Advanced bioreactor with controlled application of multi-dimensional strain for tissue engineering. J. Biomed. Eng. **124,** 742, 2002.
68. Cooper, J.A., Lu, H.H., Ko, F.K., Freeman, J.W., and Laurencin, C.T. Fiber-based tissue-engineered scaffold for ligament replacement: design considerations and *in vitro* evaluation. Biomaterials **26,** 1523, 2005.
69. Kubo, K., Kakimoto, T., Kanda, C., Tsukasa, N., Uehara, M., Izumi, Y., Kamada, T., Kaneko, N., and Sueda, T. Bioactive glass promoted formation of nodules in periodontal-ligament fibroblasts *in vitro*. J. Biomed. Mater. Res. **27,** 1175, 1993.
70. Hee, C.K., Jonikas, M.A., and Nicoll, S.B. Influence of three-dimensional scaffold on the expression of osteogenic differentiation markers by human dermal fibroblasts. Biomaterials **27,** 875, 2006.
71. Dunn, M.G., Liesch, J.B., Tiku, M.L., and Zawadsky, J.P. Development of fibroblast-seeded ligament analogs for ACL reconstruction. J. Biomed. Mater. Res. **29,** 1363, 1995.
72. Laurencin, C.T., Attawia, M.A., Elgendy, H.E., and Herbert, K.M. Tissue engineered bone-regeneration using degradable polymers: the formation of mineralized matrices. Bone **19,** 93S, 1996.
73. Marcolongo, M., Ducheyne, P., Garino, J., and Schepers, E. Bioactive glass fiber/polymeric composites bond to bone tissue. J. Biomed. Mater. Res. **39,** 161, 1998.
74. Niederauer, G.G., Slivka, M.A., Leatherbury, N.C., Korvick, D.L., Harroff, H.H., Ehler, W.C., Dunn, C.J., and Kieswetter, K. Evaluation of multiphase implants for repair of focal osteochondral defects in goats. Biomaterials **21,** 2561, 2000.
75. Ma, P.X., Zhang, R., Xiao, G., and Franceschi, R. Engineering new bone tissue *in vitro* on highly porous poly(alpha-hydroxyl acids)/hydroxyapatite composite scaffolds. J. Biomed. Mater. Res. **54,** 284, 2001.
76. Verrier, S., Blaker, J.J., Maquet, V., Hench, L.L., and Boccaccini, A.R. PDLLA/Bioglass composites for soft-tissue and hard-tissue engineering: an *in vitro* cell biology assessment. Biomaterials **25,** 3013, 2004.
77. Hench, L.L. Bioceramics: from concept to clinic. J. Am. Cera. Soc. **74,** 1487, 1991.
78. Oonishi, H., Kushitani, S., Yasukawa, E., Iwaki, H., Hench, L.L., Wilson, J., Tsuji, E., and Sugihara, T. Particulate bioglass compared with hydroxyapatite as a bone graft substitute. Clin. Orthop. **334,** 316, 1997.
79. Gatti, A.M., Valdre, G., and Andersson, O.H. Analysis of the *in vivo* reactions of a bioactive glass in soft and hard tissue. Biomaterials **15,** 208, 1994.
80. Yao, J., Radin, S., Leboy, S., and Ducheyne, P. The effect of bioactive glass content on synthesis and bioactivity of composite poly (lactic-co-glycolic acid)/bioactive glass substrate for tissue engineering. Biomaterials **26,** 1935, 2005.
81. Benjamin, M., Ralphs, J.R. Fibrocartilage in tendons and ligaments—an adaptation to compressive load. J. Anat. **193,** 481, 1998.
82. Evanko, S.P., and Vogel, K.G. Ultrastructure and proteoglycan composition in the developing fibrocartilaginous region of bovine tendon. Matrix **10,** 420, 1990.
83. Spalazzi, J.P., Gallina, J., Fung-Kee-Fung, S.D., Konofagou, E.E., and Lu, H.H. Elastographic imaging of strain distribution in the anterior cruciate ligament and at the ligament-bone insertions. J. Orthop. Res. **24,** 2001, 2006.
84. Lu, H.H., Jiang, J., Tang, A., Hung, C.T., and Guo, X.E. Development of controlled heterogeneity on a polymer-ceramic hydrogel scaffold for osteochondral repair. Bioceramics **17,** 607, 2005.
85. Yu, H., Grynpas, M., and Kandel, R.A. Composition of cartilagenous tissue with mineralized and non-mineralized zones formed *in vitro*. Biomaterials **18,** 1425, 1997.
86. Schaefer, D., Martin, I., Shastri, P., Padera, R.F., Langer, R., Freed, L.E., and Vunjak-Novakovic, G. *In vitro* generation of osteochondral composites. Biomaterials **21,** 2599, 2000.
87. Gao, J., Dennis, J.E., Solchaga, L.A., Awadallah, A.S., Goldberg, V.M., and Caplan, A.I. Tissue-engineered fabrication of an osteochondral composite graft using rat bone marrow-derived mesenchymal stem cells. Tissue Eng. **7,** 363, 2001.
88. Hollister, S.J., Maddox, R.D., and Taboas, J.M. Optimal design and fabrication of scaffolds to mimic tissue properties and satisfy biological constraints. Biomaterials **23,** 4095, 2002.
89. Woo, S.L., Gomez, M.A., Seguchi, Y., Endo, C.M., and Akeson, W.H. Measurement of mechanical properties of ligament substance from a bone-ligament-bone preparation. J. Orthop. Res. **1,** 22, 1983.

Address reprint requests to:
Helen H. Lu, Ph.D.
Department of Biomedical Engineering
Columbia University
New York, NY

E-mail: hl2052@columbia.edu